Superconductor/ferromagnet proximity effect in Fe/Pb/Fe trilayers

L. Lazar, K. Westerholt, and H. Zabel
Institut für Experimentalphysik/Festkörperphysik, Ruhr-Universität Bochum, 44780 Bochum, Germany

L. R. Tagirov
Kazan State University, 420008 Kazan, Russian Federation

Yu. V. Goryunov, N. N. Garif'yanov, and I. A. Garifullin
Kazan Physicotechnical Institute, Russian Academy of Sciences, 420029 Kazan, Russian Federation
(Received 20 May 1999; revised manuscript received 2 September 1999)

We report on measurements of structural, superconducting, and magnetic properties of trilayer and bilayer systems combined of superconducting Pb and ferromagnetic Fe. The Pb/Fe layers can be grown on Al_2O_3 with reasonably flat interfaces, there is no alloying of the components at the interface and Fe is found to be ferromagnetic down to the monolayer range. This is a favorable situation for an S/F proximity system, since it corresponds closely to the situation treated in theoretical models. We find an oscillation of the superconducting transition temperature when plotted versus the thickness of the ferromagnetic layer, which we regard as a clear indication of an unconventional, propagating superconducting pair wave function in the Pb/Fe system. We fit our results using recent theoretical model calculations and find evidence for a strongly reduced transparency of the Pb/Fe interface. We regard this as an essential feature of the proximity effect in Pb/Fe and discuss its physical origin.

I. INTRODUCTION

In recent years one notices an increasing interest in the classical proximity effect between superconducting (S) and ferromagnetic (F) thin layers.[1–10] This, on the one hand, is due to the recent progress in the preparation of high quality metallic multilayer systems and, on the other hand, motivated by the actual theoretical interest in unconventional superconducting states. Model calculations for the superconducting state in a S/F-multilayer systems indicate the possible existence of a superconducting order parameter shifting by π when crossing a ferromagnetic layer (π-wave superconductivity)[11] or the existence of a propagating character of the superconducting wave function in the ferromagnetic sublayers [Larkin-Ovshinikov-Fulde-Ferrel (LOFF) state].[12]

The most spectacular experimental result concerning the proximity effect in S/F layered systems in recent years was the observation of a $T_c(d_F)$ curve with a definite maximum when plotting the superconducting transition temperature T_c versus the thickness of the ferromagnetic layer d_F.[3,4] A superconducting T_c increasing with the thickness of the ferromagnetic layer as observed, e.g., in Nb/Gd and Nb/Fe contradicts the physical intuition, since it is expected that the strong exchange field in the ferromagnet should destroy the superconductivity.

Actually there is no consensus in the literature concerning the origin of the nonmonotonic $T_c(d_F)$ curve. First it has been interpreted as an indication of a π-wave superconducting state at the ferromagnetic layer thickness corresponding to the maximum in $T_c(d_F)$.[3] However, this conclusion turned out to be premature, since the character of the real interface in the S/F systems complicates the physical situation considerably. In most experimental S/F systems studied until now there is some alloying at the interface due to interdiffusion of the components. Thus there is no sharp S/F interface but a continuous change of the superconducting and ferromagnetic properties when crossing the interface. In the system Nb/Fe, e.g., the first ferromagnetic layer only occurs for a nominal thickness $d_{Fe}=7$ Å,[4,5] similarly, in the Nb/Gd system, the onset of ferromagnetism is observed at a nominal Gd thickness $d_{Gd}=12$ Å.[2,3] Since in both systems the onset of ferromagnetism marks the onset the nonmonotonic $T_c(d_F)$ curve, it has been concluded that the alloyed interface is essential for the structure in the $T_c(d_F)$-curve. In our previous work on Fe/Nb/Fe trilayers, we have developed a corresponding model for the explanation of the T_c maximum.[5]

In any case, the alloyed interface in S/F systems complicates the situation and has the tendency to obscure the interesting physics which is predicted for sharp S/F interfaces in the theoretical model calculations.[11] Therefore it is highly desirable to find a S/F system without alloying at the interface and a sharp onset of ferromagnetism in the range of one monolayer .

We have chosen the Pb/Fe system, guided by the very low solubility of both metals even in the liquid state[13] which suggests that interdiffusion at the interface is negligible. Actually this system was among the first in which the S/F proximity effect has been studied.[14] However, the growth properties of the Pb/Fe layered system is rather problematic and due to a rather large roughness of the interfaces, our preliminary results on the Pb/Fe samples published in Ref. 15 were rather disappointing, not showing any oscillation in the $T_c(d_{Fe})$ curve. In the meantime we were able to improve the structural quality of the Pb/Fe layered system definitely by optimizing the rf sputtering process.[16] The samples we report on here have reasonably flat interfaces and show details in the $T_c(d_{Fe})$ curve which, by comparison with model

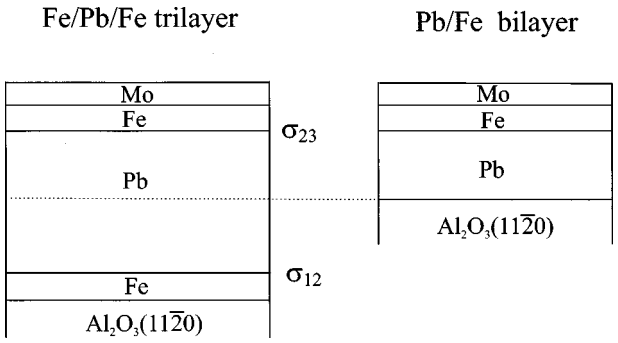

FIG. 1. Design of the samples studied. σ_{12} denotes the roughness of the interface between the first Fe layer and the Pb layer and σ_{23} is the roughness of the interface between the Pb layer and the second Fe layer.

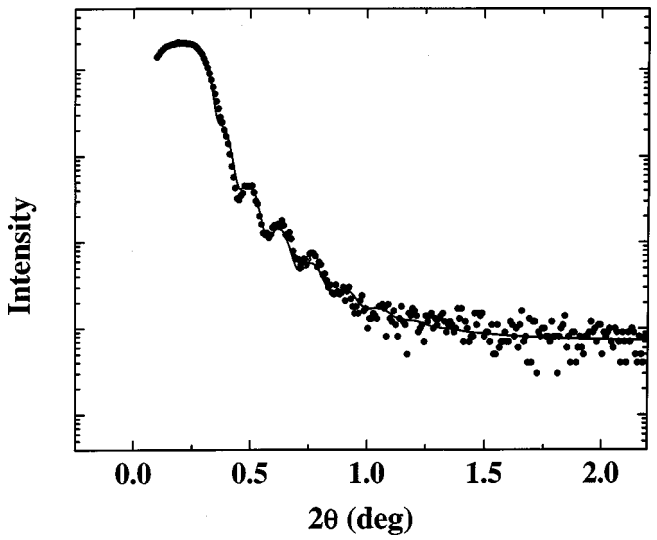

FIG. 2. X-ray reflectivity scan measured with MoK_α radiation for Pb/Fe bilayer with $d_{Fe}=30$ Å and $d_{Pb}=260$ Å prepared using optimal deposition rate for Pb 1.4 Å/s. The solid line represents a theoretical fit using the Parratt formalism (see main text).

calculations, allows deep insight into the essential features of the S/F proximity effect.

The paper is organized as follows. After a brief outline of the thin film preparation and the structural properties we present the results of the magnetization and the transport measurements.

Then we come to a further main issue of the present paper, namely, the problem of deriving the microscopic parameters determining the proximity effect by fitting the experimental results by theoretical model calculations. We first apply the theory of Radovic *et al.*,[11,17] which is established as the standard theory for the interpretation of experimental results on the S/F proximity effect in the literature. We point out an important inconsistency when applying this theory, concerning the parameter characterizing the interface. As will be shown in detail, this inconsistency can be traced back to the boundary conditions for the superconducting wave function at the S/F interface introduced by Radovic *et al.* This boundary condition implies a high quantum mechanical transparency of the S/F interface. In real systems the exchange splitting of the conduction band of the ferromagnetic layer leads to strong specular reflection of the conduction electrons. This limits the transparency of the interface drastically.

Therefore we apply a new theory for the S/F proximity effect published recently,[18] which is a generalization of the Radovic theory and takes the finite transparency of the interface explicitly into account. We show that by fitting the experimental results by this theory we get a consistent picture and can derive a realistic set of microscopic parameters, including the numerical value for the quantum mechanical transparency of the S/F interface.

II. SAMPLE PREPARATION AND CHARACTERIZATION

The samples were prepared by rf sputtering on Al_2O_3 $(11\bar{2}0)$ substrates kept at room temperature using pure Ar (99.99%) as sputter gas. The base pressure of the system was 8×10^{-8} mbar after cooling with liquid N_2. Pure Pb (99.999%) and Fe (99.99%) targets were used, the growth rate was controlled by a quartz crystal monitor. Figure 1 shows schematically the design of the Pb/Fe bilayers and Fe/Pb/Fe trilayers prepared for the present work. All samples were covered by a protective Mo cap layer of about 50 Å thickness. We studied the possibility of using of Au, Al, and Mo as materials for the protective layer and found by Auger electron spectroscopy analysis that complete covering of the Fe layer can only be achieved using Mo.

Since in the experimental sections below we are interested in the systematic change of the superconducting properties when the thickness of the Fe layers varies on a scale of several Fe monolayers, the existence of flat layers and of interfaces with a small roughness is essential. We found that the growth rate for Pb is the most important parameter determining the roughness of the interfaces.[16] The optimal growth rate for preparation of films with a small surface and interface roughness depends on the design of the samples. For the Fe/Pb bilayers starting with Pb on Al_2O_3 (right hand side of Fig. 1) the optimal growth rate is 1.4 Å/s, for Fe/Pb/Fe trilayers, i.e., with Pb growing on Fe (left hand side of Fig. 1) the optimal growth rate is 0.7 Å/s. For the sputtering of Fe a much lower growth rate of 0.1 Å/s is optimal.[19] As an example proving that actually Fe/Pb bilayers can be prepared with very flat interfaces we show in Fig. 2 a small angle x-ray reflectivity scan using MoK_α radiation of a bilayer prepared with the optimal growth conditions. One observes well resolved and weakly damped film thickness oscillations. The reflectivity spectrum has been fitted numerically by the Parratt formalism[20] generalized by Nevrot and Croce[21] in order to include the electron density height fluctuations at the interface. The fit gives a roughness parameter σ characterizing the mean thickness of the mixed interlayer of 3 Å. The low angle x-ray scattering of the Fe/Pb/Fe trilayers revealed that the bottom interface σ_{12} (see Fig. 1) has a similar small roughness parameter of about 3 Å, whereas the top interface σ_{23} has a much larger roughness parameter of about 30 Å (for details see Lazar *et al.*[16]). However, this roughness parameter σ_{23} mainly reflects the geometrical roughness of the Pb film grown on Fe. The top Fe film on Pb grows in a rather flat mode, as evidenced by the FMR measurements discussed below. The features characterizing the roughness of the Fe/Pb films by the x-ray reflectivity study are corroborated

TABLE I. Series number, layer thicknesses d_{Pb} and d_{Fe} and residual resistivity ratio (RRR) for the samples of the present study.

No.	Sample type	d_{Pb} (Å)	d_{Fe} (Å)	RRR
S749	Al_2O_3/Fe/Pb/Fe	730	0–52	9.3–10
S742		620	0–30	9.8–11
S724		740–2400	30	8.8–11
S808		750–3000	30	5.6–8.4
S809	Al_2O_3/Pb/Fe	375–1500	30	5.2–6.8

by atomic force microscopy measurements.[16] In addition, x-ray Bragg reflection measurements we made to characterize the crystalline quality of the films. For the samples with Pb grown on Fe the Pb layer is polycrystalline, for Pb grown directly on Al_2O_3, the Pb layer is single crystalline with the (111) layer in the film plane. A rocking scan at the Pb(111) Bragg reflection reveal an out-of-plane mosaicity of 0.048°.

For a precise determination of the thickness dependence of the magnetic and superconducting properties on d_{Fe} or d_{Pb}, it is essential that one series of samples is deposited under identical experimental conditions. In our experimental setup a series of nine samples were prepared within one single run. For the preparation of the Fe/Pb/Fe trilayers with variable d_{Fe} and constant d_{Pb} a shutter system was first opened completely for the simultaneous evaporation of Fe on all nine substrates arranged in an array. After a fixed time the shutter for the first sample was closed, then for the second one and so on with a fixed interval between the closing time for each subsequent sample. When the evaporation of Fe was finished, all substrate shutters were opened simultaneously for the evaporation of the Pb layer. Afterwards the process for the evaporation for the top Fe layer was repeated in the same fashion as for the bottom layer. The preparation of Fe/Pb/Fe trilayers with constant d_{Fe} and variable d_{Pb} was achieved in a similar manner. The precision for the determination of the absolute thickness of the layers from the sputtering rate or by the fitting the small angle x-ray reflectivity spectra is about 5%. The precision which can be given for the variation of the relative thickness within one series of samples, which is more important in the following sections, is much higher, namely about 1%.

For the present investigation we prepared five series of samples. The layer sequence, the thickness of the single layers and the residual resistivity ratio are summarized in Table I.

III. FERROMAGNETISM OF THE IRON LAYER

We used measurements of the magnetization by a SQUID magnetometer and ferromagnetic resonance (FMR) in order to characterize the ferromagnetism of the thin Fe films. As stated in the Introduction the development of the ferromagnetism with the Fe-layer thickness is important to characterize the S/F proximity effect.

A. Magnetization

The static ferromagnetic magnetization M at $T=20$ K is measured with the magnetic field in the film plane. The ferromagnetic hysteresis loops exhibit a square shape typical for thin Fe films without any noticeable change with varying Fe thickness. The saturation magnetization at 2 kOe is plotted versus the nominal Fe thickness d_{Fe} in Fig. 3 for the Fe/Pb/Fe trilayers of the series S749 (see Table I). Within the limits of the experimental error bars the magnetization is independent of the thickness of the Fe layer down to at least $d_{Fe}=10$ Å. The slight upturn of the $M(d_{Fe})$ curve below $d_{Fe}=10$ Å should not be taken seriously, since there is an increasing relative uncertainty in the determination of d_{Fe} for very thin layers. The constant ferromagnetic saturation magnetization coinciding with the bulk value of Fe (Fig. 3) should be contrasted by the strongly thickness dependent magnetization obtained, e.g., in Fe/Nb.[4] This result clearly indicates that Fe is ferromagnetic down to the monolayer range in the Fe/Pb system and alloying at the interface is negligible.

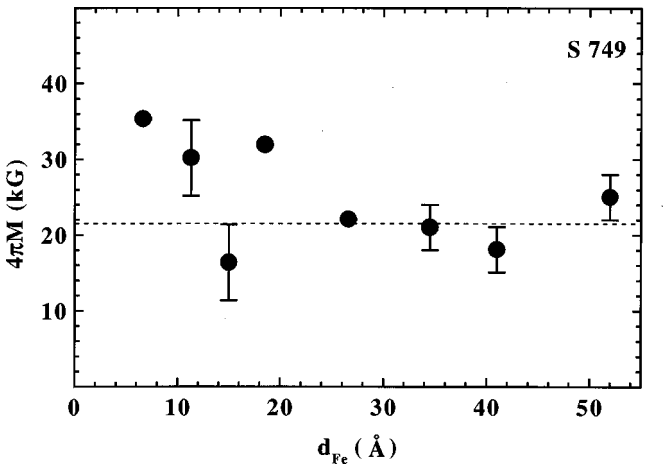

FIG. 3. Saturation magnetization versus the Fe-layer thickness d_{Fe} for the serie S749 with fixed Pb-layer thickness $d_{Pb}=730$ Å measured by a SQUID magnetometer at $T=20$ K. The dashed line indicates the bulk magnetization of Fe.

B. Ferromagnetic resonance

FMR measurements also possess a sufficient sensitivity to study very thin Fe layers. We performed FMR measurements at the frequency 9.4 GHz at room temperature. As described in detail in Ref. 16 two FMR signals can be observed for the Fe/Pb/Fe trilayers. One signal exhibits a twofold anisotropy when the magnetic field direction is rotated in the film plane. It belongs to the Fe film grown directly on sapphire $(11\bar{2}0)$ which is stongly textured with the crystallographic (110) plane parallel to the layer surface.[19] The second signal is isotropic and belongs to the polycrystalline Fe layer on top of the Pb film.

The dependence of the isotropic FMR line parameters on the thickness of the Fe layer for the Fe/Pb/Fe trilayers from the series S742 is characterized in Fig. 4. Qualitatively the thickness dependence of the parameters for the anisotropic signal is similar. With decreasing d_{Fe} the FMR resonance field H_0 [Fig. 4(a)] and the FMR linewidth ΔH [Fig. 4(b)] both increase monotonically below $d_{Fe}=15$ Å. The increase of H_0 is due to a decreasing value of the effective magnetization M_{eff}. M_{eff} is determined by the saturation magnetization M and the uniaxial perpendicular anisotropy $2K_u/M$ by the relation[22]

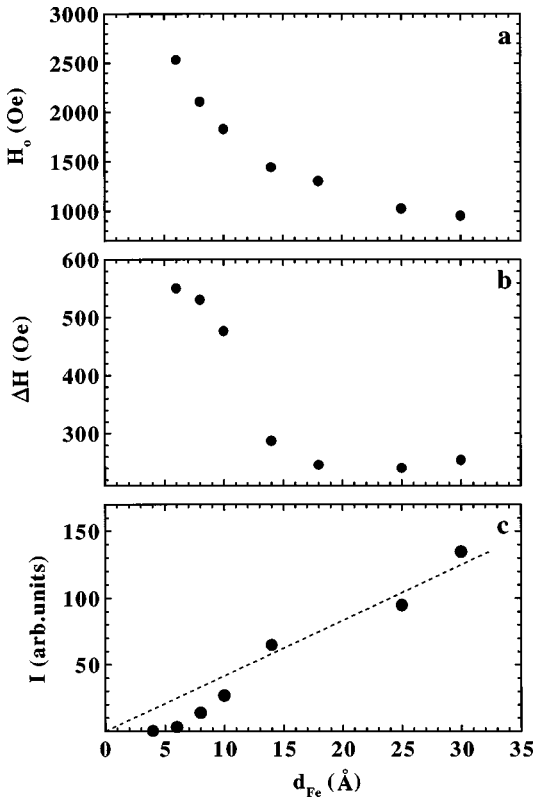

FIG. 4. FMR line position (a), linewidth (b), and intensity (c) versus the Fe-layer thickness d_{Fe} for the series S742 with fixed $d_{\mathrm{Pb}}=620$ Å.

$$4\pi M_{\mathrm{eff}}=4\pi M-\frac{2K_u}{M}, \tag{1}$$

where K_u is the out-of-plane uniaxial anisotropy constant, which usually is inversely proportional to d_{Fe}.[22] The broadening of the FMR line below $d_{\mathrm{Fe}}=15$ Å and the disappearance of the resonance signal at $d_{\mathrm{Fe}}=4$ Å probably results from the dispersion of the demagnetizing field, which appears due to the finite roughness of the Fe layer.[23] This conclusion is supported by the fact that the line broadening of the anisotropic FMR signal, which belongs to the Fe layer with smaller roughness, occurs only below $d_{\mathrm{Fe}}=10$ Å. Figure 4(c) shows the decrease of the integral intensity I of the FMR signal with decreasing d_{Fe}. The dashed line indicates the expected decrease of I due to the decreasing volume of the ferromagnetic layers. The deviation from the straight line for $d_{\mathrm{Fe}}<15$ Å is caused by the dispersion of demagnetizing field at low d_{Fe}.

IV. TRANSPORT AND SUPERCONDUCTING PROPERTIES

In this section we report on measurements of the electrical resistivity, the superconducting transition temperature T_c and the upper critical magnetic field perpendicular to the film plane $H_{c2\perp}(T)$. The resistivity was measured in a standard four terminal configuration by a low frequency ac technique with the current and voltage leads attached to the sample by silver epoxy. The superconducting transition temperature was defined as the midpoint of the transition curve. The upper critical magnetic field was also measured resistively. In addition, ac magnetic susceptibility measurements were used to determine T_c. In this case the temperature corresponding to half the value of the maximum transition signal was defined as T_c.

A. Electrical resistivity

In contrast to the situation for Nb/Fe films,[5] the T_c value and the residual resistivity ρ_0 of sputtered Pb thin films are not very sensitive to the preparation conditions. Nevertheless we observed that the samples prepared at the optimal growth conditions have the highest residual resistivity ratio $RRR=R(300\ \mathrm{K})/R_0\simeq 10$ (see Table I). Using $\rho(300\ \mathrm{K})=21\times10^{-6}\ \Omega\,\mathrm{cm}$[24] we obtain $\rho_0\simeq 2\times10^{-6}\ \Omega\,\mathrm{cm}$ for the residual resistivity. From this value we can calculate the diffusion coefficient D_s of the conduction electrons which we need in the next section for a quantitative analysis of the proximity effect. In order to estimate the diffusion coefficient D_s in Pb we use the Pippard relations[25]

$$\sigma=e^2S\langle l\rangle/12\pi^3\hbar,\quad \gamma=k_B^2S/12\pi\hbar\langle v_F\rangle, \tag{2}$$

where σ denotes the electrical conductivity, γ the electronic specific heat coefficient, v_F the Fermi velocity of conduction electrons, and l the mean free path of conduction electrons. S is the Fermi surface area and the brackets mean averaging over the Fermi surface. Combining relations (2), one obtains

$$v_F l=(\pi k_B/e)^2(\sigma/\gamma). \tag{3}$$

This relation permits an estimate of $v_F l$ from the low temperature conductivity σ and the coefficient of the electronic specific heat γ. For our sample using $\gamma=3\times10^{-3}$ J/K^2 mole for Pb,[24] we find $v_{Fs}l_s\simeq 2.3\times10^2$ cm^2/s.

For a single Fe film prepared at conditions identical to the Fe layer in our trilayers we obtained an $RRR=9$. Using $\rho(300\ \mathrm{K})=10\times10^{-6}\ \Omega\,\mathrm{cm}$ for Fe (Ref. 24) we get $\rho_0\simeq 1.1\times10^{-6}\ \Omega\,\mathrm{cm}$ and taking $\gamma=5\times10^{-3}$ J/K^2 mole for Fe,[24] we derive $v_{Fm}l_m\simeq10^2$ cm^2/s for the Fe film.

B. Upper critical magnetic field

In order to determine the coherence length in the Pb film, which is also needed for the quantitative analysis in the next section, we performed measurements of the upper critical field $H_{c2\perp}(T)$ for a single 700 Å Pb film prepared under identical conditions. The Pb films with $d_{\mathrm{Pb}}<1600$ Å are type II superconductors.[26] As expected for a three-dimensional superconductivity, our measurements (Fig. 5) give a linear temperature dependence of $H_{c2\perp}(T)$ near T_c:

$$H_{c2\perp}(T)=H_{c2\perp}(0)(1-T/T_c) \tag{4}$$

with $H_{c2\perp}(0)=4.5$ kOe. In the framework of the Ginzburg-Landau theory $H_{c2\perp}(0)$ for a superconducting film is given by $H_{c2\perp}(0)=\phi_0/2\pi\xi_{\mathrm{GL}}^2(0)$ with ϕ_0 being the flux quantum and ξ_{GL} the Ginzburg-Landau coherence length. $H_{c2\perp}(0)$ value of 4.5 kOe yields a coherence length $\xi_{\mathrm{GL}}(0)\simeq 260$ Å. The superconducting coherence length ξ_s used in Ref. 11 is related to the Ginzburg-Landau coherence length $\xi_{\mathrm{GL}}(T)$ via

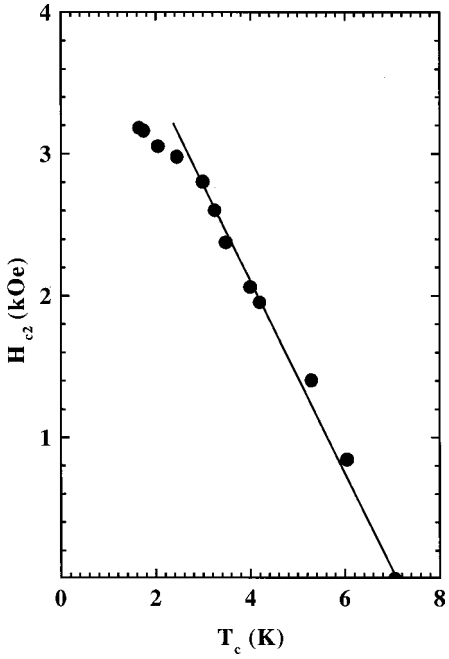

FIG. 5. Temperature dependence of the upper critical field for an orientation of the magnetic field perpendicular to the film plane vs T for a single uncovered Pb film with $d_{\mathrm{Pb}}=700$ Å.

$$\xi_{\mathrm{GL}}(T)=\frac{\pi}{2}\xi_s(1-T/T_c)^{-1/2}, \tag{5}$$

giving $\xi_s \simeq 170$ Å.

C. Proximity effect

Figure 6 shows examples for the superconducting transitions observed by electrical resistivity and ac magnetic susceptibility measurements for four samples from the series S724 with different d_{Pb} (see Table I). The widths of the transitions are typically 0.1 K, confirming the high quality of our films.

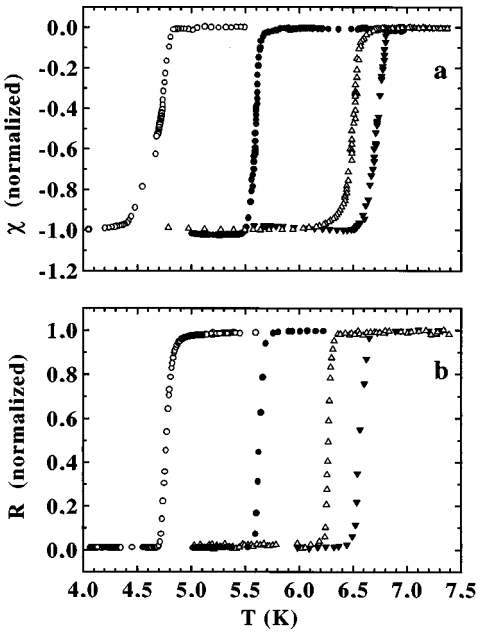

FIG. 6. Superconducting transition curves measured by ac susceptibility (a) and electrical resistivity (b) for the series S724 with $d_{\mathrm{Pb}}=2400$ Å (closed triangles), 1800 Å (open triangles), 1240 Å (closed circles), 960 Å (open circles).

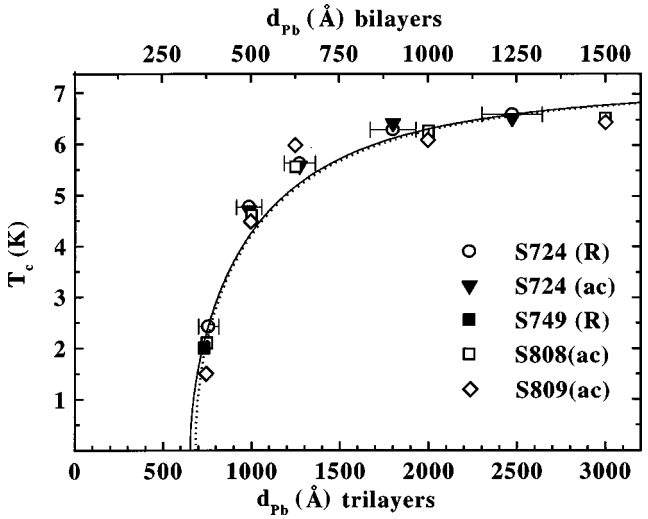

FIG. 7. Dependence of the superconducting transition temperature on the thickness of the Pb-layer for four sample series listed in Table I. The dotted and solid lines are the best fits using the theory by Radović *et al.* and the theory by Tagirov, respectively, with parameters given in the figure subscripts of Figs. 10 and 11.

Figure 7 summarizes one central experimental result of the present paper, namely, the dependence of the superconducting transition temperature on the thickness of the Pb layer d_{Pb} with the thickness of the Fe layer fixed at 30 Å. The diagram combines measurements of four series of samples from Table I measured resistively or by ac susceptibility. All transition temperatures fall on one universal curve, confirming the good reproducibility of the results. One should note that the diagram in Fig. 7 contains measurements on three Fe/Pb/Fe trilayer systems and one bilayer system Pb/Fe with exactly half the thickness for the Pb layer compared to the trilayers. From symmetry considerations this scaling should be expected, since in the trilayer system the Cooper pairs are subjected to pair breaking from the exchange field of two Fe layers and in the bilayer only of one Fe layer. The scaling also gives confidence that from the point of view of the proximity effect both Fe/Pb interfaces are identical, although crystallographically and structurally they are different (see Secs. II and III). An important influence of a possible oxidation of the interfaces or the Fe layer, which should be much stronger for the top Fe layer and the top interface, can also be excluded from the scaling behavior of $T_c(d_{\mathrm{Pb}})$ in Fig. 7. An additional confirmation of this conclusion can be obtained from Fig. 8 where the superconducting transition curves for trilayers (series S808) and bilayers (series S809) measured using the ac magnetic susceptibility, are presented. It can clearly be seen that the shape and the width of the transition curves for the trilayers and for the corresponding bilayers (with a factor of 2 smaller Pb thicknesses) are almost the same. In case of different Pb/Fe and Fe/Pb interface qualities one would expect a much broader superconducting transitions for the trilayers as compared to bilayers.

As will be discussed in detail in the next section, the experimental points in Fig. 7 can be fitted by theoretical

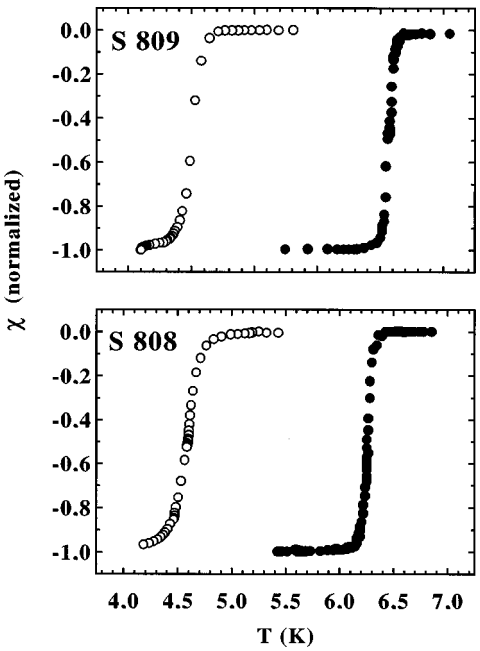

FIG. 8. Superconducting transition curves are compared for bilayers and trilayers. The upper panel reproduces ac-susceptibility measurements for bilayers (S809) with $d_{Pb}=1000$ Å and $d_{Pb}=500$ Å, the lower panel for trilayers (S808) with $d_{Pb}=2000$ Å and $d_{Pb}=1000$ Å. In both sets the Fe-layer thickness is $d_{Fe}=40$ Å.

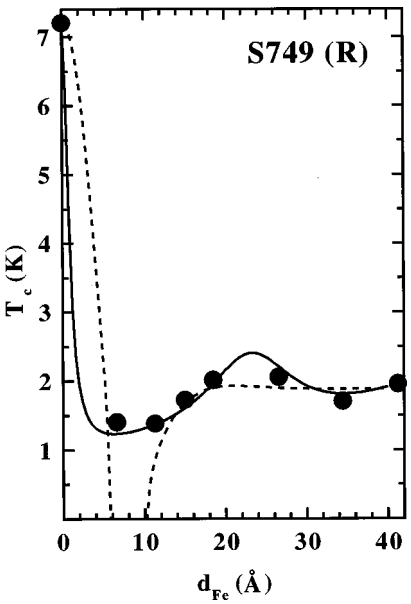

FIG. 9. Dependence of the superconducting transition temperature on the thickness of the Fe layer as determined by resistivity measurements (closed symbols) for the series S749 (see Table I). The dashed and solid lines are the best fits using the theory by Radović *et al.* and the theory by Tagirov, respectively, with parameters given in the figure subscripts of Figs. 10 and 11.

curves (lines in the figure) thus allowing the determination of microscopic parameters. For the time being, we only point out that we derive a critical thickness $d_{Pb}^{crit}\simeq 700$ Å for Fe/Pb/Fe trilayers and $d_{Pb}^{crit}\simeq 350$ Å for the bilayers for the vanishing of superconductivity.

The second essential result of the present paper is shown in Fig. 9 where we have plotted the dependence of the superconducting transition temperature T_c versus the thickness of the Fe layer with the thickness of the Pb layer fixed at 730 Å. T_c drops sharply when increasing d_{Fe} up to $d_{Fe}=6$ Å, passes through a flat minimum with $T_c\simeq 1.4$ K, increases slightly by about 0.5 K and saturates at about 2 K. The width of the superconducting transitions for this series of samples does not exceed 0.1 K. Therefore error bars in determination of T_c is of the order of 0.05 K. As mentioned in the second section, the error bars in the thickness of the Fe layers within one series of samples can be estimated to be below 1 Å and thus are within the experimental points plotted in Fig. 9. The roughness parameters of the Fe layers determined by the small angle x-ray scattering measure the thickness fluctuations on a very small lateral length scale. Since we do not observe any broadening of the superconducting transition curve in resistivity or ac-susceptibility, the lateral length scale of the thickness fluctuations seems to be smaller than the superconducting coherence length. In this case the roughness parameter is irrelevant for the $T_c(d_{Fe})$ curve in Fig. 9. In addition our SQUID-magnetization and FMR data indicate that Fe layers in our samples are continuous at least down to 6 Å. This means that in spite of some roughness of the surfaces, the local thickness of the Fe layer is more or less constant within the whole area of the film. Thus we regard the existence of the minimum in the $T_c(d_{Fe})$ curve as well established experimentally in Fig. 9. As mentioned in the Introduction, oscillations in the $T_c(d_{Fe})$ curve is the most interesting aspect in the S/F proximity effect, and, referring to the theory, are a hallmark for unconventional superconductivity in these systems. We have observed this effect in the Pb/Fe system. For the samples with a larger roughness parameters ($\sigma_{23}>50$ Å) the $T_c(d_{Fe})$ curve turned out to be a monotonically decreasing function.[15]

V. DISCUSSION

We now come to the interpretation of the experimental results, especially the thickness dependencies $T_c(d_{Pb})$ (Fig. 7) and $T_c(d_{Fe})$ (Fig. 9) in the framework of theoretical calculations. In most of the previous experimental studies the theory by Radović *et al.*[11,17] was applied and we will also analyze our experimental data first using their theory. Within the single-mode approximation the reduced superconducting transition temperature $t_c=T_c/T_{c0}$ (where T_{c0} is the transition temperature for the isolated superconducting layer) can be found as a solution of the equation [see Eq. (7) in Ref. 17]

$$\mathrm{Re}\,\Psi\left(\frac{1}{2}+\frac{\rho}{t_c}\right)-\Psi\left(\frac{1}{2}\right)+\ln(t_c)=0, \tag{6}$$

where $\mathrm{Re}\,\Psi(x)$ means the real part of the digamma function $\Psi(x)$. The pair breaking parameter for a trilayer is defined as

$$\rho=\frac{2\phi^2}{(d_s/\xi_s)^2}, \tag{7}$$

where $\phi=k_s d_s/2$, ξ_s is the superconducting coherence length and k_s is the propagation momentum of the pairing wave function in the superconducting layer, which can be

found from the boundary conditions at the outer surfaces of the trilayer and the matching of the solutions at the S/F interfaces.

In the dirty limit for the superconductor and in close vicinity of T_c the pairing function $F_{s,m}$ is given by the linearized Usadel equations[27] which have to be solved for the $F/S/F$ trilayer making use of the boundary conditions introduced by Ivanov *et al.*[28] at $x=\pm d_s/2$:

$$\frac{dF_s}{dx}=\eta\frac{dF_m}{dx}, \tag{8}$$

$$F_s=F_m. \tag{9}$$

The absence of the pairing function current through the outer surfaces of the trilayer implies that at $x=\pm(d_s/2+d_m)$

$$\frac{dF_m}{dx}=0. \tag{10}$$

From the derivation of the boundary condition (8) in Ref. 28 the parameter η in Eq. (8) is given by $\eta=\sigma_m/\sigma_s$, i.e., the ratio of the normal state conductivities of the ferromagnetic and superconducting layers.

Using the boundary conditions (8), (9), and (10) the equation for computing ϕ in Eq. (7) can be derived:[18]

$$\phi\tan\phi=\frac{k_m\xi_m}{2\varepsilon}\left(\frac{d_s}{\xi_s}\right)\tanh(k_m d_m) \tag{11}$$

with

$$\varepsilon=\frac{\xi_m}{\eta\xi_s},\quad \xi_m=\left(\frac{4\hbar D_m}{|I|}\right)^{1/2},\quad D_m=\frac{1}{3}v_{Fm}l_m,\quad k_m^2=\frac{2iI}{\hbar D_m}. \tag{12}$$

Here ξ_m is the penetration depth of the superconducting pairing function into the ferromagnet, D_m is the diffusion constant in the ferromagnet and I is the exchange splitting of the conduction band in the ferromagnet.

The set of equations (6), (7), and (11) are the basic equations of the theory of Radović *et al.* for $F/S/F$ trilayers. In the paper of Radović *et al.*[11] the multimode solution (exact numerical solution) for the superconducting layer has been presented. A numerical investigation of the single-mode approximation in Ref. 18 showed that the exact and the single-mode solutions coincide asymptotically at $d_s>2\xi_s$, where d_s is the thickness of the superconducting layer in the $F/S/F$ trilayer. This result is expected physically, because the single-mode propagation momentum k_s represents the longest mode with a range $\sim\xi_s$, higher order modes are essentially short-range modes and strongly damped at $d_s\gg\xi_s$. As we intend to employ the analysis to Fe/Pb/Fe trilayers with $d_s/\xi_s>2$, the single mode solution is a good approximation.

The $T_c(d_{\mathrm{Pb}})$ curve in Fig. 7 shows that the citical thickness $d_{\mathrm{Pb}}^{\mathrm{crit}}$ below which superconductivity vanishes is $d_{\mathrm{Pb}}^{\mathrm{crit}}\simeq 700$ Å for the trilayer. From the measurements of the upper critical field we get $\xi_s\simeq 170$ Å, thus the superconductivity vanishes at $d_s/\xi_s\simeq 4$. Sets of $T_c(d_s)$ curves calculated using Eqs. (6), (7), and (11) for the case $d_m/\xi_m\gg 1$ and different ε values give $\varepsilon\simeq 3.4$. The dotted line plotted in Fig. 7 is the theoretical $T_c(d_s)$ curve corresponding to this ε value.

In the next step we fit theoretical $T_c(d_{\mathrm{Fe}})$ curves to the experimental results in Fig. 9. The experimental points exhibit a broad minimum at $d_{\mathrm{Fe}}\simeq 8$ Å. Theoretical $T_c(d_{\mathrm{Fe}})$ curves calculated using Eqs. (6), (7), and (11) show that the minimum in $T_c(d_m)$ curve, which physically is caused by the interference of the Cooper pair wave function reflected from the surfaces of the ferromagnetic layers, occurs at $d_m/\xi_m\simeq 0.5$. Thus from the position of the minimum in the $T_c(d_{\mathrm{Fe}})$ dependence (Fig. 9) we determine the penetration depth of the Cooper pairs into the ferromagnetic layer $\xi_m\simeq 16$ Å.

The dashed line in Fig. 9 shows the theoretical curve corresponding to the values of $\xi_m=16$ Å and $\varepsilon=3.4$. The overall structure of the $T_c(d_{\mathrm{Fe}})$ curve is reproduced approximately, but instead of a shallow minimum the theory predicts the reentrant behavior of the superconductivity. However, one should note that the theoretical curve is idealistic in the sence that it neglects any roughness of the surface and interface, does not consider spin-orbit scattering, which can be rather strong at the interface,[15] and neglects inelastic pair breaking scattering in the ferromagnet.[18] All these properties are poorly defined in the experimental system, but, as model calculations demonstrate, have the tendency to smooth the deep minimum at $d_m/\xi_m\simeq 0.5$ and suppress the reentrant behavior of the superconducting state. However, the position of the minimum at $d_m/\xi_m=0.5$ and the saturation value of T_c at $d_m\gg\xi_m$ are independent of these additional complications in the real systems to a good approximation and thus can be taken seriously when comparing experiment and theory. Keeping these restrictions in mind, one gains the impression that the model by Radović *et al.* appears to describe the experimental results rather satisfactorily.

However, from the parameter $\varepsilon=\xi_m/\eta\xi_s=3.4$ obtained in the fit we can estimate the parameter of the theory η [see Eq. (8)], which characterizes the Pb/Fe interface. Using $\xi_m\simeq 16$ Å and $\xi_s\simeq 170$ Å we obtain $\eta\simeq 0.03$. This very low value for the parameter η is characteristic for all systems when fitting the Radović theory. For instance, for V/Fe $\eta=0.013$ has been obtained,[1] for Nb/Gd Strunk *et al.* obtained $\eta=0.047$,[2] in our previous work on Fe/Nb we have derived $\eta\sim 0.02$.[5] As mentioned above, within the microscopic model by Ivanov *et al.*[28] the parameter η is equal to the ratio of normal state conductivities $\eta=\sigma_m/\sigma_s$. Taking our measurements of the residual resistivities $\rho_0=2\times 10^{-6}$ Ω cm for the Pb layer and $\rho_0=1.1\times 10^{-6}$ Ω cm for the Fe layer, we get $\eta=1.8$ which is a factor of 50 larger than η derived above. The discrepancy is obvious and striking.

Figure 10 shows the spatial variation of the real part of the pairing wave function F near the interface with the parameters obtained in our fitting. At the S side the function $\mathrm{Re}\,F_s$ decreases slightly as the interface is approached. When crossing the interface the derivative of F function increases by a factor η^{-1}, giving a steep decrease of F_m at the F side of the interface. At larger distances from the interface F_m exhibits the oscillatory behavior with a change of sign at $d_m\sim 0.5\xi_m$. The main peculiarity in the behavior of the pairing function is the sharp drop of F_m near the interface caused by the small η value.

There is another hidden discrepancy between our experimental data and the theory of Radović *et al.* If one assumes, as it is done within the Radović theory, that the pairing function is continuous at the interface (i.e., assuming a perfectly

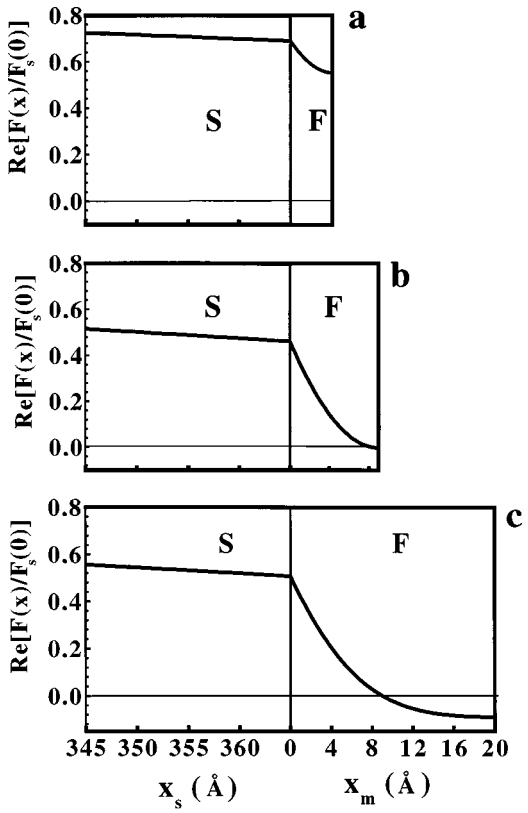

FIG. 10. Spatial variation of the real part of the pairing function near the interface in the model by Radović *et al.* for the series S749 with $d_{\mathrm{Pb}}=730$ Å and $d_{\mathrm{Fe}}=4$ Å (a), 9 Å (b), and 20 Å (c) with the parameters $\xi_s=170$ Å, $\xi_m=16$ Å, and $\varepsilon=3.4$ as obtained by the fit.

transparent interface) and neglects any influence of spin-orbit interaction, the T_c suppression can be easily estimated quantitatively. The exchange splitting of the conduction band in Fe, $2I_{\mathrm{Fe}}$, is about 1 eV (see, e.g., Ref. 1, and references therein). In the Cooper limit, which is sufficient as a rough estimate, the effective exchange field acting on the Cooper pairs in the Fe layer is given by its value averaged over the total thickness of the Fe/Pb/Fe trilayer

$$I_{\mathrm{eff}}\simeq 2I_{\mathrm{Fe}}\frac{2d_{\mathrm{Fe}}}{d_{\mathrm{Pb}}+2d_{\mathrm{Fe}}}. \tag{13}$$

Then we consider the Clogston limit for the spin splitting of the conduction band, i.e. the field $H=\sqrt{2}\Delta/g\mu_B$ which completely quenches superconductivity. With the gap parameter $\Delta=1.76k_BT_c\simeq 1.2$ meV for Pb and the exchange field estimated as $H=I_{\mathrm{eff}}/g\mu_B$, a complete quenching of superconductivity is expected for $d_{\mathrm{Fe}}\sim 0.5$ Å. This corresponds to less than one monolayer and is in strong contradiction to the experimental result in Fig. 9 where we find that superconductivity survives up to $d_{\mathrm{Fe}}\sim 40$ Å. This second severe contradiction demonstrates that there is an essential shortcoming in the theory which makes it unrealistic for a quantitative comparison to experimental systems. We will argue in the following that this shortcoming is the high transparency of the interface assumed in the theory.

Aarts *et al.*[6] were the first who shed light on the important role of the interface transparency and presented experimental evidence of the intrinsically reduced interface transparency in the $V/V_{1-x}Fe_x$ multilayer system. They discussed their experimental results using the boundary conditions in the dirty limit for the S/F interface, which have been derived by Kupriyanov and Lukichev[29] from the general boundary conditions for the quasiclassic Green functions by Zaitsev.[30] The first boundary condition is Eq. (8), which ensures the continuity of the electric current associated with charged quasiparticles crossing the interface, the second boundary equation (9) at $x=\pm d_s/2$ is replaced by

$$-D_m(\mathbf{n_m}\cdot\nabla F_m)=\frac{v_mT_m}{2}(F_s-F_m), \tag{14}$$

where $\mathbf{n_m}$ is the unit vector perpendicular to the interface and T_m is the dimensionless interface transparency parameter ($T_m\in[0,\infty]$):

$$T_m=\int_0^1 dt\,\frac{tT(t)}{1-T(t)}, \tag{15}$$

$T(t)$ denotes the angle-dependent quantum mechanical coefficient of transmission through the interface, $t=\cos\theta$, where θ is the angle between the interface normal and the trajectory of the transmitted electron. The key qualitative difference between the boundary condition (9) used by Radović *et al.* and the modified one in Eq. (14) is that the latter allows a jump of the anomalous Green function at the interface, while Eq. (9) assumes that the pairing function is continuous across the interface. In other words, the boundary condition (14) explicitly takes the finite transparency of the S/F interface for the Cooper pairs into account.

Now, using the boundary conditions (8), (10), and (14) and taking the renormalization of the diffusion coefficient in the F layer[31] into account, one obtains a new basic equation for finding ϕ in Eq. (7)[18,32]

$$\phi\tan\phi=\frac{1}{2}\left(\frac{N_m}{N_s}\right)\left(\frac{D_m^+}{D_s}\right)\frac{(k_m^+d_s)\tanh(k_m^+d_m)}{1+(2D_m^+k_m^+/T_mv_m)\tanh(k_m^+d_m)}, \tag{16}$$

where

$$k_m^+=\frac{2iI+\tau_s^{-1}}{D_m^+} \tag{17}$$

with

$$D_m^+=\frac{1}{3}\,\frac{v_{Fm}l_m}{1+2iIl_m/v_{Fm}}. \tag{18}$$

Here N_m and N_s is the density of states of the conduction electrons at the Fermi level in the ferromagnetic and superconducting layer, respectively. The complex value of the diffusion coefficient D_m^+ reflects the inhomogeneous character of the pairing state in the exchange-split conduction band of a ferromagnet. The inhomogeneous pairing function experiences pair breaking with characteristic scattering time τ_s depending on the I value[18] due to spin independent potential scattering of electrons. Now the transition temperature of the $F/S/F$ trilayer is determined by the solution of the set of

Eqs. (6), (7), and (16), and depends on the transparency of the interface via the parameter T_m (15).

In the case of the perfect quantum mechanical interface transparency for the parameter T_m in Eq. (14) $T_m \gg 1$ holds. In this limit and reasonable values of other parameters the second term in the denominator of Eq. (16) can be neglected. Then making use of the definition of $\eta = \sigma_m/\sigma_s = (N_m D_m/N_s D_s)$ in Eq. (16) and neglecting the renormalization in D_m^+, we reproduce exactly the previous equation of Radović (11), which turns out to be the high transparency limit of Eq. (16). We thus conclude that the theory by Radović *et al.* can be expected to provide a quantitative model for an experimental system only in the case of perfect interface transparency ($T_m \gg 1$).

If, as in most experimental systems, the S/F interface transparency is not very high we have to use the general equation (16) for the calculation of ϕ in Eq. (7). In this case the parametrization of the basic equations (6), (7) and (16) via the coherence length ξ_s, the magnetic stiffness length $\xi_I = v_{Fm}/2I$, the mean free path of conduction electrons in the ferromagnetic layer l_m, the interface transparency parameter T_m and the ratio $(N_m v_{Fm}/N_s v_{Fs})$ appears to be natural.

At the first glance, due to the large number of parameters the fitting of this theory to the experimental data looks rather arbitrary. However, combining all experimental results which we have and considering restrictions limiting the range of validity of several parameters, one is able to fit a realistic set of parameter values. First, the coherence length ξ_s has been determined from the upper critical field measurements. Next we regard the limit $d_m \gg \xi_I$ which imposes restrictions on the possible values of T_m and $(N_m v_{Fm}/N_s v_{Fs})$. In the limit $t_c \to 0$ at $d_m \gg \xi_I$ using Eqs. (7) and (16) we obtain for the critical thickness of the superconducting layer from Eq. (6):

$$d_s^{\mathrm{crit}} = 2\sqrt{2\gamma}\,\xi_s \arctan\left[\frac{\pi}{\sqrt{2\gamma}}\frac{\xi_{\mathrm{BCS}}}{\xi_s}\frac{(N_m v_m/N_s v_s)}{1+2/T_m}\right]. \quad (19)$$

Equation (19) is valid for an arbitrary transparency parameter T_m and $l_m \gg \xi_I$ (see discussion of the latter inequality in Ref. 18). Using $d_s^{\mathrm{crit}} = 700$ Å for our Fe/Pb/Fe trilayer system, $\xi_s = 170$ Å as derived above and the BCS coherence lenth of Pb $\xi_{\mathrm{BCS}} = 830$ Å,[24] from Eq. (19) we obtain

$$\left(\frac{N_m v_{Fm}}{N_s v_{Fs}}\right)\frac{1}{1+2/T_m} \simeq 0.22. \quad (20)$$

Numerical analysis shows that the $T_c(d_s)$ curve hardly depends on l_m. At the same time the $T_c(d_m)$ dependence is very sensitive to the variation of the T_m and l_m, allowing to determine l_m and the pairs T_m and $(N_m v_{Fm}/N_s v_{Fs})$, confined by Eq. (20). As can be seen from Figs. 3 and 5 of Ref. 18 the superconducting transition temperature exhibits oscillatory behavior as a function of the ferromagnetic layer thickness d_m. The first minimum in $T_c(d_m)$ curve occurs at $d_m \sim 0.5\xi_I$ for $T_m > 5$. With decreasing the T_m below $T_m \sim 5$ the minimum shifts to a smaller magnetic layer thickness. The T_m value affects mainly the region of the first minimum of the $T_c(d_m)$ curve. The value of l_m, in contrast, mainly influences the oscillation amplitude in the $T_c(d_m)$ curve. The shape of the minimum of $T_c(d_{\mathrm{Fe}})$ in Fig. 9 yields $T_m = 0.4$, thus corresponding with Eq. (20) to $N_m v_{Fm}/N_s v_{Fs} \simeq 1.3$. The oscillation amplitude gives $l_m/\xi_I \sim 2$ as an estimate, the position of the maximum gives $\xi_I \simeq 7.7$ Å, corresponding to $l_m \simeq 15$ Å. Actually, we regard the existence of an oscillation in $T_c(d_{\mathrm{Fe}})$ with a maximum at $d_{\mathrm{Fe}} \sim 20$ Å as not clearly proven, regarding the experimental points alone. However, the theoretical curve suggests that an oscillation exists and the drop of T_c for the sample with $d_{\mathrm{Fe}} = 34$ Å is definitely outside of the experimental error bar. So the optimum strategy for fitting the experimental results is to control the shape of the minimum by T_m, the height of the shoulder by l_m while rescaling d_m by ξ_I to ensure the correct position of the minimum and the shoulder.

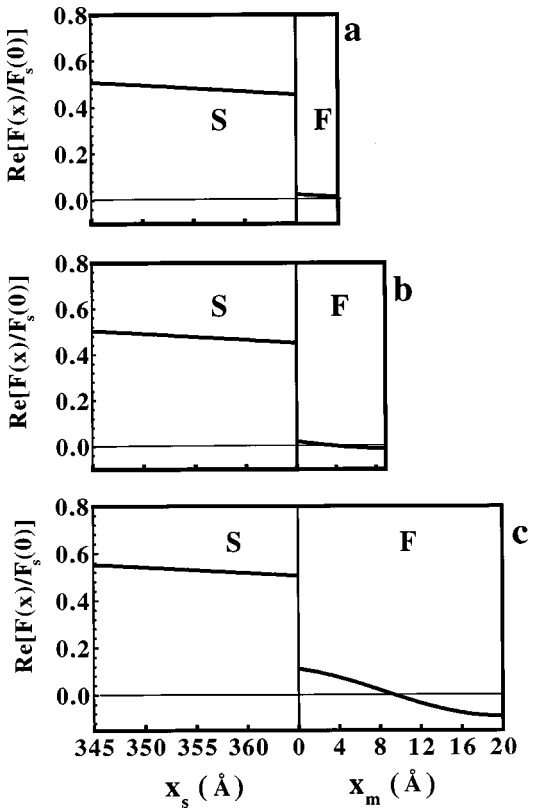

FIG. 11. Spatial variation of the real part of the pairing function near the interface in the model by Tagirov for the series S749 with $d_{\mathrm{Pb}} = 730$ Å and $d_{\mathrm{Fe}} = 4$ Å (a), 9 Å (b), and 20 Å (c) with the parameters $\xi_s = 170$ Å, $\xi_I = 7.7$ Å, $l_m = 15$ Å, $N_m v_{Fm}/N_s v_{Fs} = 1.3$ and $T_m = 0.4$ as obtained by the fit.

A fit of the experimental results with the set of parameters obtained following this strategy is plotted as a solid line in Figs. 7 and 9. The numerical values of the parameters are given in the subscript of Fig. 11. The quality of the fit is satisfactory, including details in the $T_c(d_{\mathrm{Fe}})$ structure in Fig. 9. This means that the position of the maximum which gives ξ_I is determined correctly.

We want to comment shortly on the qualitative features of the pairing wave function on the ferromagnetic side in Fig. 11. The amplitude and phase of the wave function in the F layer results from an interference of the incident wave function and the wave function reflected at the ferromagnet/vacuum interface. The situation is not intuitively clear and the wave function must be calculated numerically by solving

the wave equations with respect to the specific boundary conditions and the kinetic transparency. The main experimental manifestation of the oscillating pairing wave function on the *F*-side is the evident minimum in the $T_c(d_{\mathrm{Fe}})$ curve, possibly followed by a strongly damped further oscillation. The theoretical analysis[18] shows that the existence of minimum in the $T_c(d_m)$ curve is very robust feature against any perturbations which destroy the interference of the pairing function in the *F* layer.

Next we want to discuss critically the numerical values of the parameters. Using the values for the Fermi velosity $v_{Fm} \sim 10^8$ cm/s and the splitting of conduction band in Fe $2I \sim 1$ eV (see, e.g., Ref. 1, and references therein), we obtain $\xi_I = \hbar v_{Fm}/2I \sim 6$ Å which agrees well with ξ_I value obtained from our fit.

The value for the electron mean free path $l_m \sim 15$ Å is considerably lower than $l_m \sim 100$ Å which we have obtained from our resistivity data using again $v_{Fm} \sim 10^8$ cm/s. We believe that this discrepancy can be resolved as follows: The electric current in a ferromagnet with exchange split subbands is carried by two parallel, spin-up and spin-down, spin channels, which do not mix at low temperatures and can exhibit strongly differing conductivities.[33] In resistivity measurements the highly conductive channel shunts the low conductive one, thus one essentially measures the long mean free path of the highly conductive channel. In contrast, in the proximity effect theory l_m plays the role of a decay length of the pairing function in the ferromagnetic layer (at $l_m \gg \xi_I$). Since the Cooper pairs consist of two quasiparticles from both subbands it is plausible to assume that the shorter path dominates in the decay length. Since the difference in the mean free path can be a factor of 5 and larger,[34] the discrepancy seems plausible. One should also bear in mind that the value of l_m obtained by our fitting procedure will increase when introducing a nozero value for τ_s^{-1}.[18] In our fit we took $\tau_s^{-1} = 0$ because its value cannot properly be determined from the experiment.

The spatial variation of the pairing function calculated with the set of parameters derived here is depicted in Fig. 11. The main difference between the behavior of the pairing function obtained within the model by Radović *et al.* (Fig. 10) and the new model is the definite jump of the *F* function at the interface. We now find $\eta = 0.5$ for the parameter defined in Eq. (8) compared to $\eta = 0.028$ derived within the theory of Radović. Since $\eta = \sigma_m/\sigma_s$ is the ratio of the normal state conductivities, $\eta = 0.5$ seems reasonable.

The above results should convince the reader that a consistent interpretation of the experimental data can be achieved within the framework of a proximity effect theory, which takes explicitly the finite transparency of the *S*/*F* interface into account. The transparency parameter $T_m = 0.4$ derived here is considerably reduced as compared to $T_m \simeq 10-15$, which ensures the applicability of the Buzdin-Radović perfect transparency limit from the general set of equations (6), (7), and (16).

The transparency parameter T_m entering in the proximity theory may vary within the range $[0,\infty]$. It is not suitable to compare it with the quantum mechanical transmission coefficient obtained via *S*/*F* tunneling or point contact spectroscopy, which lies in the range [0, 1]. Equation (15) suggests the following parametrization of the transparency parameter T_m:

$$T_m = \frac{\overline{T}}{1-\overline{T}}, \tag{21}$$

where $\overline{T}$ denotes the angular averaged quantum mechanical transmission coefficient of the interface and $0 < \overline{T} < 1$. In contrast to a similar single-parametric characterization of the interface transparency by Aarts *et al.*, $\overline{T}$ thus defined does not depend on the film properties such as l_m or ξ_m, but only on the transmission properties of the interface. With $T_m = 0.4$ derived from our proximity effect experiments we obtain from Eq. (21) $\overline{T} = T_m/(1+T_m) = 0.29$, which is considerably reduced with respect to the ideally transparent interface having $\overline{T} = 1$.

The microscopic origin of the strongly reduced interface transparency needs to be explained. We believe that, the exchange splitting of the conduction band in the ferromagnet is the main physical reason. In fact, the spin polarization of the conduction band of a ferromagnet introduces a difference between the transmission probabilities through an *S*/*F* interface for quasiparticles with spin-down ($T_\downarrow$) and spin-up ($T_\uparrow$). It is natural to suppose that the transmission coefficient for the Cooper pairs in the *S*/*F* proximity effect theory is close to the smaller one of the two transparency coefficients $T_\uparrow$ and $T_\downarrow$ for quasiparticles forming Cooper pairs. Quantum mechanical reflection of quasiparticles due to Fermi momentum mismatch takes place for quasiparticles incident on the interfaces. For example, electrons for which the projection of the momentum parallel to the interface $k_\parallel$ satisfies the condition $k_{F1} < k_\parallel < k_{F2}$ (k_{F1} and k_{F2} being the two Fermi vectors), experience complete internal reflection from the side of the larger k_F, thus decreasing the phase space of electrons responsible for the mutual influence of the ferromagnetic and superconducting layers.

We expect an additional decrease of the $\overline{T}$ value due to a chemical mismatch of Pb and Fe giving rise to a contact potential barrier at the interface. The barrier height is determined by the difference in the work functions of both materials.[35] This barrier leads to a weak hybridization of the Pb and Fe derived wave functions at the interface. We expect that the barrier height is larger for immiscible metals, such as Pb and Fe in comparison to metals which are soluble similar to V and Fe, or form intermetallic compounds such as Nb and Fe. This will further reduce the transparency of the *S*/*F* interface and the amplitude of the pairing function in the ferromagnetic layer.

Finally, it is worthwhile to compare the transmission coefficient derived from proximity effects with direct measurements of the transmission coefficients using tunneling or point contact spectroscopy. These measurements also point towards a possible strong reduction of the transmission coefficients $T_\uparrow$ and $T_\downarrow$ of the quasiparticles through the *F*/*S* interface.[36,37] For example, the authors of Ref. 37 deduced a transmission coefficient $T_\downarrow$ for the spin-down electrons of $T_\downarrow \simeq 0.38$ for Co/Pb and $T_\downarrow \simeq 0.43$ for Ni/Pb, as compared to $T_\downarrow \simeq 0.79$ for Cu/Pb. This demonstrates the substantial reduc-

tion of the transmission probabilities for ferromagnetic materials compared to nonmagnetic materials.

Electronic energy band structure calculations taking the band matching and the complicated Fermi surface into account allow a first principle calculations of transmission and reflection coefficients of F/N interfaces such as Ag/Fe, Au/Fe, Cu/Co, and Cu/Ni.[38] These calculations, too, demonstrate the strong spin dependence of these quantities. The transmission probabilities averaged over the Fermi surface lie in the range of 0.14–0.38 for the minority spin states transmitted from the ferromagnetic to the nonmagnetic side, and in the range of 0.16–0.8 for the reverse direction. The calculations clearly reveal the physical origin of the low transmission of the interface: (1) weak hybridization of some electronic states due to symmetry restrictions, (2) internal reflection for the part of the Fermi surface where the momentum parallel to the interface does not match, and (3) complete reflection for certain areas of the Fermi surface if the sizes of the Fermi spheres are different. The third reason can be expressed as a Fermi-momentum mismatch at the interface. Due to the complex nature of the energy bands the transmission probability usually varies strongly over the area of the interface Brilloun zone. Nevertheless, as a rule, the strongly reduced average transparency of the interface especially for the minority electrons at N/F boundaries is clearly evident from the calculations. Thus both, point contact spectroscopy and band structure calculations for the N/F interfaces support our conclusion about the low interface transparency of the Pb/Fe interface.

VI. SUMMARY AND CONCLUSIONS

In the first part of this paper we presented a detailed experimental study of the proximity effect in the Pb/Fe layered system. The growth of flat layers is rather problematic in this system, but bilayers and trilayers can be grown on sapphire substrates with sufficient structural quality. At very low Fe-layer thickness of only few Å, the FMR-results indicate a possible discontinuous ferromagnetic film. The proximity effect, however, averages over the lateral magnetic inhomogeneities on a length scale of the superconducting correlation length, so the superconducting transitions remain sharp even in this thickness range. As expected from the alloy phase diagram of the Fe-Pb system, there is no alloying of the elements at the interfaces and the Fe layers are ferromagnetic down to the monolayer thickness. Comparing different S/F material combinations used for the study of the proximity effect up to now, the Pb/Fe layer system fulfills best the theoretical assumption of a sharp interface.[11,17,18] We find oscillations in the $T_c(d_{\mathrm{Fe}})$ curve, which we regard as a clear indication of the existence of an unconventional, propagating pairing state in the ferromagnetic sublayers of Pb/Fe. As mentioned in the Introduction, in the Nb/Gd and Nb/Fe systems, where an oscillating $T_c(d_{\mathrm{Fe}})$ has been observed previously,[3,4] the situation is not at all clear due to the complex influence of the alloyed interfaces.

In the second part of the paper we concentrated on the analysis of the $T_c(d_{\mathrm{Fe}})$ and $T_c(d_{\mathrm{Pb}})$ curves obtained for the Pb/Fe layer system using two different theoretical models. When fitting the more recent model,[18] which is a generalization of the pioneering work by Radovic *et al.*,[11] we got a consistent interpretation of the experimental results and could derive important and otherwise poorly defined microscopic parameters such as like the exchange stiffness length and the effective interface transparency.

A comparison of the fitting parameters obtained within the two models also revealed the origin of an inconsistency which has often been encountered when applying the Radovic *et al.* model to experimental systems: The assumption of a highly transparent interface, which is implicitly contained in this model, is not justified in most systems studied until now. A fit with the parameters of the model leads to an unrealistically high gradient of the pairing wave function on the ferromagnetic side of the interface which mimics the discontinuity in the pairing wave function actually occurring in real systems. The possibility of a reduced and strongly spin dependent interface transparency in systems composed of ferromagnetic and normal metal has been recognized in recent years in connection with the problem of the giant magnetoresistance.[38] It is caused by quantum mechanical reflection of the conduction electrons at the interface due to electron energy band mismatch.

We find that the transmission coefficient of the Pb/Fe interface has a remarkably low value, comparable to the typical values derived for the minority spin electrons in other S/F systems. This low transparency leads to a strongly reduced mixing of the superconducting and ferromagnetic electron systems and is the basic reason for the fact that the superconductivity in the thin Pb layers survives up to a rather large thickness of the Fe layer. We argued that the low transparency of the Pb/Fe interface for the quasiparticles is on the one hand due to the weak hybridization of the Pb- and Fe-wave functions and on the other hand due to the exchange splitting of the Fe-conduction band, combined with the fact that the decay length of the superconducting pairing function in the ferromagnet is mainly determined by the lower of the two spin dependent transmission coefficients.

ACKNOWLEDGMENTS

The authors would like to thank Professor G.G. Khaliullin for his participation in this study during the early stage, and for fruitful discussion of the results at the final stage. The support of this work by the Deutsche Forschungsgemeinschaft (Grant No. DFG-ZA 161/16-1) and by the Russian Fund for Fundamental Research (Project No. 99-02-17393), is gratefully acknowledged. One of us (I.A.G.) acknowledges NATO support under Grant No. HTECH.EV 972833.

[1] P. Koorevaar, Y. Suzuki, R. Coehoorn, and J. Aarts, Phys. Rev. B **49**, 441 (1994).
[2] C. Strunk, C. Sürgers, U. Paschen, and H.v. Löhneysen, Phys. Rev. B **49**, 4053 (1994).
[3] J.S. Jiang, D. Davidović, D.H. Reich, and C.L. Chien, Phys. Rev. Lett. **74**, 314 (1995).
[4] Th. Mühge, N.N. Garif'yanov, Yu.V. Goryunov, G.G. Khaliullin, L.R. Tagirov, K. Westerholt, I.A. Garifullin, and H. Zabel, Phys. Rev. Lett. **77**, 1857 (1996).
[5] Th. Mühge, K. Westerholt, H. Zabel, N.N. Garif'yanov, Yu.V. Goryunov, I.A. Garifullin, and G.G. Khaliullin, Phys. Rev. B **55**, 8945 (1997).
[6] J. Aarts, J.M.E. Geers, E. Brück, A.A. Golubov, and R. Coehoorn, Phys. Rev. B **56**, 2779 (1997).
[7] J.E. Mattson, C.D. Potter, M.J. Conover, C.H. Sowers, and S.D. Bader, Phys. Rev. B **55**, 70 (1997).
[8] Th. Mühge, N.N. Garif'yanov, Yu.V. Goryunov, K. Theis-Bröhl, K. Westerholt, I.A. Garifullin, and H. Zabel, Physica C **296**, 325 (1998).
[9] G. Verbanck, C.D. Potter, V. Metlusko, R. Schad, V.V. Moschalkov, and Y. Bruynseraede, Phys. Rev. B **57**, 6029 (1998).
[10] C. Attanasio, C. Coccorese, L.V. Mercaldo, M. Salvato, L. Maritano, A.N. Lykov, S.L. Prischepa, and C.M. Falco, Phys. Rev. B **57**, 6056 (1998).
[11] Z. Radović, M. Ledvij, L. Dobrosavljević-Grujić, A.I. Buzdin, and J.R. Clem, Phys. Rev. B **44**, 759 (1991).
[12] A.I. Larkin and Yu.N. Ovchinnikov, Zh. Éksp. Teor. Fiz. **47**, 1136 (1964) [Sov. Phys. JETP **20**, 762 (1965)]; P. Fulde and R.A. Ferrel, Phys. Rev. **135**, A550 (1964).
[13] O. Kubaschewski, *Iron-Binary Phase Diagrams* (Springer-Verlag, Berlin, 1982), p. 87.
[14] J.J. Hauser, H.C. Theuerer, and N.R. Werthamer, Phys. Rev. **142**, 118 (1966).
[15] N. N. Garif'yanov, Yu.V. Goryunov, Th. Mühge, L. Lazar, G.G. Khaliullin, K. Westerholt, I.A. Garifullin, and H. Zabel, Eur. Phys. J. B **1**, 405 (1998).
[16] L. Lazar, K. Westerholt, H. Zabel, Yu. V. Goryunov, and I. A. Garifullin, Thin Solid Films (to be published).
[17] Z. Radović, L. Dobrosavljević-Gruji, A. I. Buzdin, and J.R. Clem, Phys. Rev. B **38**, 2388 (1988).
[18] L.R. Tagirov, Physica C **307**, 145 (1998).
[19] Th. Mühge, A. Stierle, N. Metoki, H. Zabel, and U. Pietsch, Appl. Phys. A: Solids Surf. **59**, 659 (1994).
[20] L.G. Parratt, Phys. Rev. **95**, 359 (1954).
[21] L. Névot, and P. Croce, Rev. Phys. Appl. **15**, 761 (1980).
[22] B. Heinrich and J.F. Cochran, Adv. Phys. **42**, 523 (1999).
[23] C. Chappert and P. Bruno, J. Appl. Phys. **64**, 5736 (1988).
[24] C. Kittel, *Introduction to Solid State Physics* (Wiley, New York, 1976), p. 266.
[25] A.B. Pippard, Rep. Prog. Phys. **23**, 176 (1960).
[26] G.J. Dolan, J. Low Temp. Phys. **15**, 133 (1974).
[27] K. Usadel, Phys. Rev. Lett. **25**, 507 (1970).
[28] Z.G. Ivanov, M.Yu. Kuprianov, K.K. Likharev, S.V. Meriakri, and O.V. Snigirev, Sov. J. Low Temp. Phys. **7**, 274 (1981).
[29] M.Yu. Kuprianov and V.F. Lukichev, Sov. Phys. JETP **67**, 1163 (1988).
[30] A.V. Zaitsev, Sov. Phys. JETP **59**, 1015 (1984).
[31] Physical reason for this renormalization is described in details by E.A. Demler, G.B. Arnold, and M.R. Beasley, Phys. Rev. B **55**, 15 174 (1997).
[32] Similar equation has been obtained independently by M.G. Khusainov and Yu.N. Proshin, Phys. Rev. B **56**, 14 283 (1997).
[33] M.B. Stearns, J. Magn. Magn. Mater. **104-107**, 1747 (1992); J. Appl. Phys. **73**, 6396 (1993).
[34] B. Dieny, J. Magn. Magn. Mater. **136**, 335 (1994).
[35] R.E. Camley and R.L. Stamps, J. Phys.: Condens. Matter **5**, 3727 (1993).
[36] R.J. Soulen, Jr., J.M. Byers, M.S. Osofsky, B. Nadgorny, T. Ambrose, S.F. Cheng, P.R. Broussard, C.T. Tanaka, J. Novak, J.S. Moodera, A. Barry, and J.M.D. Coey, Science **282**, 85 (1998).
[37] S.K. Upadhyay, A. Palanisami, R.N. Louie, and R.A. Buhrman, Phys. Rev. Lett. **81**, 3247 (1998).
[38] M.D. Stiles, J. Appl. Phys. **79**, 5805 (1996).